

Metallic Nature of the Four-Dimensional Quantum Hall Edge

Y. D. Chong and R. B. Laughlin

Department of Physics, Stanford University, Stanford, California 94309

(Dated: November 5, 2018)

We study the density response of the four-dimensional quantum Hall fluid found by Zhang and Hu, which has been advanced as a model of emergent relativity. We calculate the density-density correlation function along the edge at half-filling, and show that it is similar to the three-dimensional free electron gas. This indicates that the edge of the four-dimensional quantum Hall fluid behaves like a metal.

PACS numbers: 71.10.Ca, 73.20.Mf, 73.43.-f

Zhang and Hu have recently discovered a beautiful four-dimensional generalization of the quantum Hall state [1, 2]. The relevance of this model to nature is the potential for emergent relativity at its edge. Were there such an effect, the magnetic length—a scale implicit in all Landau-level structures—would form a natural ultraviolet cutoff for the system, potentially producing a quantum-mechanical description of the vacuum of space-time that is internally consistent at all length scales, something that presently does not exist. To this end, Zhang and Hu discussed a set of special particle-hole pair excitations obeying the “equations of motion” of massless relativistic bosons. However, it is quite misleading to describe the boson dispersion relation in this way, because these objects are not real particles unless something stabilizes them against decay into their fermionic components [3]. There are two strong reasons to suspect that this is not the case. One is that the model consists fundamentally of noninteracting fermions filled up to a Fermi energy. Since the density of states at the Fermi energy is nonzero, the low-temperature specific heat of the model is linear in the temperature, and thus vastly larger than any relativistic system could possibly have; a relativistic model in 3 spatial dimensions has a specific heat rising as T^3 if it is massless, and exponentially activated if it has mass. The second point is that the fermions flow towards potential minima in just the way electrons in a metal do; this is, in fact, a key assumption of Zhang and Hu’s analysis. The key properties of the model thus indicate that it is not a relativistic vacuum, but a new kind of metal.

In order to clarify this matter, we have calculated the model’s density-density response function numerically. The result is shown in Fig. 1. It may be seen that this response function is so much like that of a noninteracting Fermi sea that the two are *impossible to distinguish* at low frequencies and long wavelengths. This suggests that the Zhang-Hu model is a metal, albeit one lacking a conventional Fermi surface and therefore of a type not previously known, and that the “relativistic bosons” identified by Zhang and Hu are modes of compressional sound.

The Zhang-Hu model describes noninteracting

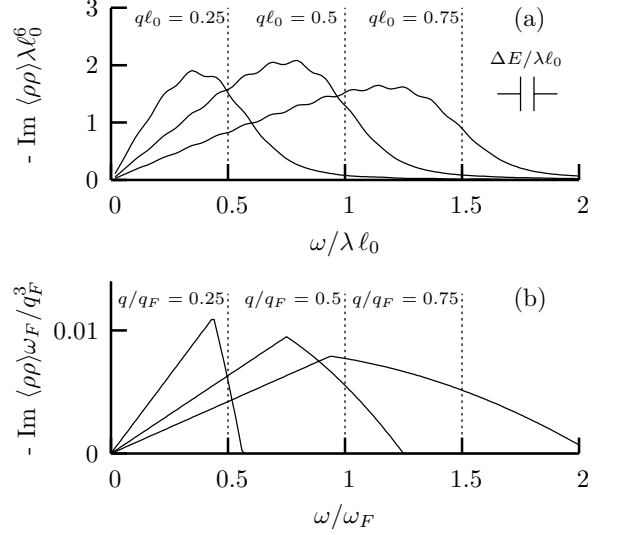


FIG. 1: Plots of $-\text{Im}\langle \rho_q \rho_{-q} \rangle_\omega$ against ω . (a) The 4D quantum Hall edge (Eq. (15)), with $\eta = 0.087 \lambda \ell_0$, $\alpha = 1$, and $p = 300$. q and ω are scaled against the natural units $1/\ell_0$ and $\lambda \ell_0$. Dotted lines are the threshold frequencies $\omega = 2(q\ell_0)(\lambda \ell_0)$. The wiggles in the curves are due to fact that the excitation energies are discrete (the energy quantum $\Delta E = [2\sqrt{p}/(p+4)]\lambda \ell_0$ is marked), which go to a continuum as $p \rightarrow \infty$. (b) The three-dimensional free electron gas (Eq. (16)), with ω and q scaled against the Fermi frequency and wave vector respectively. Dotted lines show the frequencies $\omega = cq$, where $c = 2\omega_F/q_F$ is the Fermi velocity.

fermions of isospin $p/2$ placed on the surface of a sphere in five spatial dimensions. Position on the sphere is specified by coordinates $x = (x_1, \dots, x_5)$, which one normalizes to the sphere radius: $\sum_{a=1}^5 x_a^2 = 1$. The Hamiltonian is

$$\mathcal{H} = -\frac{1}{2} \sum_{a < b} (x_a D_b - x_b D_a)^2 + \lambda x_5 \quad (1)$$

where $D_a \equiv \partial_a + a_a$ and λx_5 is a perturbative confining potential. The vector potential a_a is generated by a Yang

monopole [4],

$$a_\mu = \frac{-i}{2(1+x_5)} \eta_{\mu\nu}^i x_\nu I_i \quad , \quad a_5 = 0 \quad (2)$$

$$\eta_{\mu\nu}^i = \epsilon_{i\mu\nu 4} + \delta_{i\mu} \delta_{4\nu} - \delta_{i\nu} \delta_{4\mu}$$

where I_i are SU(2) isospin operators satisfying $[I_i, I_j] = i\epsilon_{ijk} I_k$. The ‘‘strength’’ of the monopole is characterized by the eigenvalue of $I^2 = I_1^2 + I_2^2 + I_3^2$, which is $p/2(p/2 + 1)$.

The natural length scale is the magnetic length, given by $\ell_0 \equiv 1/\sqrt{p}$. Zhang and Hu work in the thermodynamic limit $p \rightarrow \infty$, meaning the magnetic length vanishes compared to the sphere radius. The natural energy scale is $\lambda\ell_0$, the confining potential energy at one magnetic length.

The isospin degree of freedom is conveniently parameterized by coherent-state spinor coordinates $u_1 = \cos(\theta/2)e^{i\phi/2}$, $u_2 = \sin(\theta/2)e^{-i\phi/2}$ [5]. In this representation, the isospin operators have the form

$$I_+ = u_1 \frac{\partial}{\partial u_2} \quad I_- = u_2 \frac{\partial}{\partial u_1} \quad I_3 = \frac{1}{2} (u_1 \frac{\partial}{\partial u_1} - u_2 \frac{\partial}{\partial u_2}). \quad (3)$$

In the absence of a confining potential ($\lambda = 0$), the energy eigenstates of this Hamiltonian in the lowest Landau level are all degenerate and given by

$$\langle x, u | m \rangle = \sqrt{\frac{p!}{m_1! m_2! m_3! m_4!}} \Psi_1^{m_1} \Psi_2^{m_2} \Psi_3^{m_3} \Psi_4^{m_4} \quad (4)$$

where $m_1 + m_2 + m_3 + m_4 = p$ and

$$\begin{pmatrix} \Psi_1 \\ \Psi_2 \end{pmatrix} = \sqrt{\frac{1+x_5}{2}} \begin{pmatrix} u_1 \\ u_2 \end{pmatrix} \quad (5)$$

$$\begin{pmatrix} \Psi_3 \\ \Psi_4 \end{pmatrix} = \frac{x_4 - ix_i \sigma_i}{\sqrt{2(1+x_5)}} \begin{pmatrix} u_1 \\ u_2 \end{pmatrix},$$

with σ_i denoting the Pauli matrices. We abbreviate the set of four quantum numbers by $m = \{m_1, m_2, m_3, m_4\}$ and denote these states by $|m\rangle$.

In the presence of a confining potential, these wavefunctions continue to be eigenstates to linear order in λ , but the degeneracy is partially broken because they are centered at different latitudes. The energy eigenvalue of $|m\rangle$ is $E_m = \lambda \langle m | x_5 | m \rangle$, where

$$\langle m | x_5 | m \rangle = \frac{m_1 + m_2 - m_3 - m_4}{p + 4} \sqrt{p} \ell_0 \quad . \quad (6)$$

If the number of particles N is less than the Landau level degeneracy $(p+1)(p+2)(p+3)/6$, the confining potential causes the particles to puddle at the bottom of the sphere. The multi-particle ground state is then a Slater determinant of single-particle states having $\langle x_5 \rangle$ up to some ‘‘Fermi latitude’’ x_5^F . The edge of the puddle, given by $x_5 = x_5^F$, is a three-dimensional space. With N fixed, multi-particle excited states are constructed by

introducing particle-hole pairs, with hole states centered below the Fermi latitude and particle states above it. We ignore excitations involving states in higher Landau levels, which is permissible since the confining potential is weak.

The density-density response function [6] describes the changes to the particle density that result from perturbing the system with weak potentials, and is effectively the Ohm’s law conductivity. Analogies to the conventional Ohm’s law must be drawn carefully here because the appropriate conserved particle current is non-Abelian. The density-density response function describes only the longitudinal conductivity measured, for example, in an electron energy-loss experiment in aluminium film. This kind of experiment also makes sense in the Zhang-Hu model because the number of fermions is conserved. The idea is to apply a time-dependent perturbation Hamiltonian $\Delta\mathcal{H}(t) = \int V(x_0, t) \rho(x_0) d^4x_0$, where $\rho(x_0) = \sum_{j=1}^N \delta^4(x_0 - x_j)$ is the density operator; solve $i\hbar \partial_t |\psi(t)\rangle = [\mathcal{H} + \Delta\mathcal{H}(t)] |\psi(t)\rangle$; and then compute the expectation value $\langle \psi(t) | \rho(x) | \psi(t) \rangle$. Note that the density operator here is four-dimensional, since the particles are constrained to lie on a four-dimensional surface. To linear order in $V(x, t)$ the result is completely specified by the density-density response function

$$\begin{aligned} \langle \rho(x) \rho(x_0) \rangle_\omega = & \sum_{\substack{\langle m | x_5 | m \rangle \leq x_5^F \\ \langle m' | x_5 | m' \rangle > x_5^F}} \left\{ \frac{\rho_{mm'}(x) \rho_{m'm}(x_0)}{(\omega + i\eta) - (E_{m'} - E_m)} \right. \\ & \left. + \frac{\rho_{mm'}(x_0) \rho_{m'm}(x)}{-(\omega + i\eta) - (E_{m'} - E_m)} \right\} \quad , \quad (7) \end{aligned}$$

where

$$\rho_{m'm}(x) = \langle m' | \delta^4(x) | m \rangle / \sqrt{\langle m' | m' \rangle \langle m | m \rangle} \quad . \quad (8)$$

The frequency ω refers to a particular Fourier component of the time-dependent potential $V(x, t)$. The ‘‘infinitesimal’’ η corresponds physically to the inverse of the experiment duration. Setting it to a small positive value slightly larger than the energy level splitting, as we do here, amounts to the constraint that the experiment never be done for a sufficiently long time to resolve this splitting. Note that states involving multiple particle-hole excitations do not contribute because their matrix elements vanish identically.

We extract the momentum dependence of the response function (7) in the following way. We first set the number of fermions N equal to the number of Landau level states for which $\langle x_5 \rangle \leq 0$ (i.e. half-filling), thus placing the edge at the equator $x_5 = 0$. The wavefunctions and matrix elements are then easy to evaluate along the great circle

$$x = (\sin \xi, \cos \xi, 0, 0, 0), \quad (9)$$

which is contained in the edge. Note that the angle ξ also gives the distance along the great circle, since lengths are normalized to the sphere radius. We find that

$$\rho_{m'm}(\xi) = \frac{g_{m'm}}{p^2 \ell_0^4} (-1)^{m_3+m_3'} \times e^{i\xi(m_3-m_4-m_3'+m_4')} \delta_{m_1+m_4}^{m_1'+m_4'} \quad (10)$$

where

$$g_{m'm} \equiv \frac{(p+2)(p+3)}{2^{p+4}\pi} \frac{(m_1+m_4)!(m_2+m_3)!}{\sqrt{m_1!..m_4!m_1'!..m_4'!}} \quad (11)$$

Note that $g_{m'm} = g_{mm'}$, as required by hermiticity of $\rho(\xi)$. For numerical purposes, it is helpful to write (7) as the Fourier series

$$\langle \rho(\xi)\rho(0) \rangle_\omega = \frac{1}{p^4 \ell_0^8} \sum_{n=-p}^p f_n(\omega) e^{in\xi} \quad (12)$$

where the coefficients f_n are given by

$$f_n(\omega) = \sum_{m,m',\pm}^{(n)} \frac{g_{m'm}^2}{\mp(\omega+i\eta) - (E_{m'} - E_m)} \quad (13)$$

with the sum taken over quantum numbers satisfying

$$\begin{aligned} m_3 - m_4 - m_3' + m_4' &= \pm n \\ m_1 + m_4 - m_1' - m_4' &= 0 \\ m_1 + m_2 - m_3 - m_4 &\leq 0 \\ m_1' + m_2' - m_3' - m_4' &> 0 \\ m_i, m_i' &\geq 0, \quad \sum m_i = \sum m_i' = p \end{aligned} \quad (14)$$

Note that this sum is invariant under the simultaneous interchange of labels (1,2) and (3,4), so that $f_n(\omega) = f_{-n}(\omega)$. The momentum-dependent response function is given in terms of these quantities by

$$\begin{aligned} \langle \rho_q \rho_{-q} \rangle_\omega &= \frac{4\pi(\sqrt{p}\ell_0)^3}{Q} \int_0^\infty \langle \rho(\xi)\rho(0) \rangle_\omega e^{-\alpha\xi^2} \sin(Q\xi) \xi d\xi \\ &= \frac{(\sqrt{p}\ell_0)^3}{Q} \left(\frac{\pi}{\alpha}\right)^{\frac{3}{2}} \sum_{n=-p}^p (Q+n) f_n(\omega) e^{-(Q+n)^2/4\alpha} \end{aligned} \quad (15)$$

where $Q \equiv q\sqrt{p}\ell_0$ and α is a convergence factor required to remove standing-wave effects on the sphere.

The need for a convergence factor is shown in Fig. 2, where we plot the untransformed response function. There is a large resonant response at the antipode $\xi = \pi$, which oscillates at the frequency of the energy quantum $\Delta E = [2\sqrt{p}/(p+4)]\lambda\ell_0$. This antipodal response occurs because even and odd n correspond to different sets of energy levels in (14), and is an artifact of the finite system size. It disappears in the thermodynamic limit, where the energy quantum goes to zero and the sphere

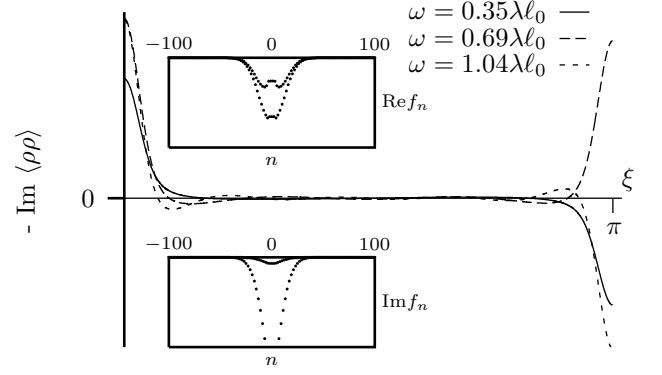


FIG. 2: Plot of $-\text{Im}\langle \rho(\xi)\rho(0) \rangle_\omega$ against ξ for different ω , generated with $p = 300$ and $\eta = 0.087\lambda\ell_0$. Inset: Fourier frequency components f_n for $\omega = 0.35\lambda\ell_0$. The two populations correspond to even and odd n , which are resonant at different frequencies.

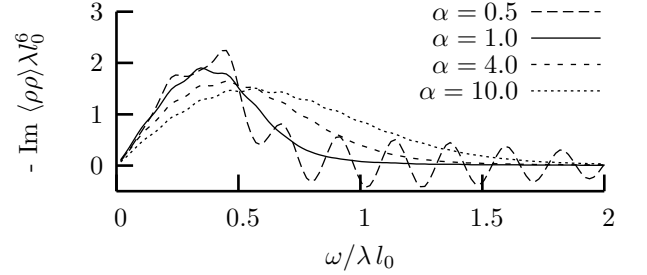


FIG. 3: Plots of $-\text{Im}\langle \rho_q \rho_{-q} \rangle_\omega$ against ω for $\eta = 0.087\lambda\ell_0$, $q\ell_0 = 0.25$, and $p = 300$.

radius goes to infinity. A similar phenomenon occurs for the 1D Fermi sea on a ring. In order to compare with the thermodynamic limit, the desired convergence factor α is the smallest one that removes the peak at the antipode, which otherwise produces a long-range ringing in the Fourier spectrum. Larger values of α would relax momentum conservation unnecessarily. It may be seen from Fig. 3 that the optimal value is about $\alpha \sim 1$. We note in particular that the response at low frequencies is diminished by increasing α , indicating that it is physical and not an artifact of α .

The calculation has been tested in several important ways. For $p \leq 4$, which was sufficiently small to allow brute-force integration over the spin angles θ and ϕ , we verified the isotropy and translational invariance of (7) and its accurate agreement with (12). The code generating the latter was then scaled up to larger values of p by changing a single parameter. We also evaluated the Fourier transform in (15) numerically and found it to accurately match the analytic version.

Returning now to Fig. 1, we observe that $\text{Im}\langle \rho_q \rho_{-q} \rangle_\omega$, as given by (15), is strikingly similar to the single-spin density-density response function for the noninteracting Fermi sea in three spatial dimensions, given by the well-

known Lindhard function [6]

$$\begin{aligned}
 -\text{Im} \langle \rho_q \rho_{-q} \rangle_\omega &= \frac{q_F^3}{16\pi\omega_F} \\
 &\times \begin{cases} \frac{\omega'}{q'}, & 0 < \omega' < 2q' - q'^2 \text{ and } q' < 2 \\ \frac{1}{q'} \left[1 - \left(\frac{\omega' - q'^2}{2q'} \right)^2 \right], & |2q' - q'^2| < \omega' < 2q' + q'^2 \\ 0 & \text{otherwise.} \end{cases} \\
 \omega' &\equiv \omega/\omega_F, \quad q' \equiv q/q_F
 \end{aligned} \tag{16}$$

In either case one finds that $\text{Im} \langle \rho_q \rho_{-q} \rangle_\omega$ is proportional to ω for small values of ω and falls to zero at a threshold frequency $\omega = cq$. In the case of the Fermi gas, c is the Fermi velocity, or, equivalently, the speed of compressional sound in the fluid. In the case of the quantum Hall edge, $c \equiv 2\lambda/p$ is the speed of the ostensibly relativistic “extremal dipoles” found by Zhang and Hu. These extremal dipoles are pair excitations which, for a given energy, have the lowest possible momentum along the edge. The non-extremal dipoles, which possess lower energies for each given momentum, produce the response

at $\omega < cq$. Elvang and Polchinski [3] have referred to the non-extremal edge states as “tachyonic states”. However, this behavior is most simply interpreted as that of a metal, in which case the extremal dipoles may be identified by analogy as conventional sound.

We wish to thank B. A. Bernevig, J. P. Hu, D. I. Santiago, and S. C. Zhang for encouragement and numerous helpful discussions. This work was supported by the Department of Energy under Contract No. DE-AC03-76SF00515. CYD acknowledges the Public Service Commission (Singapore) for support.

-
- [1] S. C. Zhang and J. P. Hu, *Science* **294**, 823 (2001).
 - [2] S. C. Zhang and J. P. Hu, *Phys. Rev. B* **66**, 125301 (2002).
 - [3] H. Elvang and J. Polchinski, hep-th/0209104.
 - [4] C. N. Yang, *J. Math. Phys.* **19**, 320 (1978).
 - [5] F. D. M. Haldane, *Phys. Rev. Lett.* **51**, 605 (1983).
 - [6] D. Pines and P. Nozières, *The Theory of Quantum Liquids* (W.A. Benjamin, 1966).